Mass spectrometric approaches to the reactivity of transient neutrals

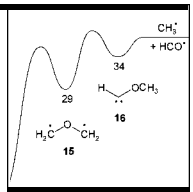

CHEMICAL SOCIETY REVIEWS

Christoph A. Schalley, Georg Hornung, Detlef Schröder and Helmut Schwarz*

Institut für Organische Chemie, Technische Universität, Straße des 17. Juni 135, 10623 Berlin, Germany

During the past few years, Neutralisation–Reionisation Mass Spectrometry (NRMS) has developed from a method for the generation and structural characterisation of elusive and highly reactive neutral molecules to a useful tool for probing their chemical reactivity. Three major principles can be distinguished: (i) peak shape analysis, (ii) activation of the neutrals by collisions or light, and (iii) variation of the neutrals' lifetimes. Several methodological approaches are discussed in conjunction with illustrating examples for the chemical reactivity of transient neutrals.

1 Introduction

The use of mass spectrometers for the examination of the unimolecular chemistry of *neutral* molecules seems, at first sight, as odd as squaring the circle, because magnetic and electrostatic fields primarily afford mass analysis of *ionic* species. However, the discovery that one-electron transfer to or from fast moving ion beams can be achieved by high energy collisions led to the development of neutralisation–reionisation mass spectrometry (NRMS), which was first applied to chemical problems almost 20 years ago.

NRMS has proved to be of enormous value for the formation of elusive and highly reactive neutrals, which are difficult to generate by other means due to their propensity toward unimolecular fragmentation or fast bimolecular rearrangements. The literature up to 1994 dealing with NRMS has been documented in several reviews.[1–8] The generation of acepentalene **1** (Scheme 1),[9] ylides such as **2** and **3**,[10] carbenes

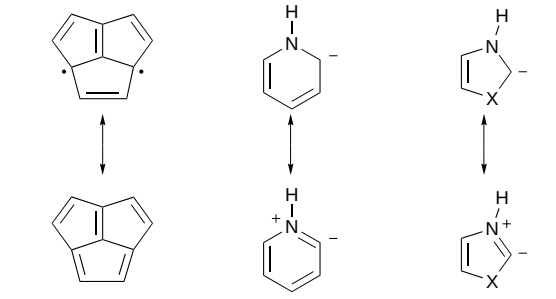

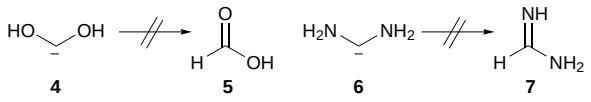

Scheme 1

like **4** and **6**, which in the gas phase do not isomerize to **5** and **7**,[11,12] and several cumulenes[13] of broad interest represent some more recent and instructive examples for the performance of

Christoph A. Schalley, born 1968 in Krefeld, Germany, studied chemistry in Freiburg and Berlin as a fellow of the Studienstiftung des Deutschen Volkes. He obtained his PhD with Professor Schwarz in 1997.

Georg Hornung, born 1966 in Zalaegerszeg, Hungary, studied chemistry in Berlin and Canterbury and is currently working on his PhD with Professor Schwarz.

Detlef Schröder, born 1963 in Wilster, Germany. He obtained his PhD with Professor Schwarz at the TU Berlin in 1992, and is currently working as research assistant in the laboratory of Professor Schwarz. He is the recipient of the 1993 Schering Award and the 1997 Mattauch-Herzog Preis.

Helmut Schwarz, born in 1943, spent four years as a chemical technician before reading chemistry at the Technische Universität Berlin (TUB), where he obtained his PhD under the supervision of F. Bohlmann in 1972 and his habilitation in 1974. Since 1978 he has been at the TUB as a Professor of Chemistry and has resisted all temptations to leave Berlin for good. He has held visiting appointments in Cambridge, Lausanne, Jerusalem, Innsbruck, Haifa, Paris, Auckland and Canberra. Among his several awards are the Otto-Klung, Otto-Bayer, and the Leibniz Prizes, and the Max-Planck Research Award, which he received jointly with C. Lifshitz. In 1992, the Hebrew University of Jerusalem conferred an honorary doctorate on him and he received in 1994 the J. J. Thompson Gold Medal. Dr Schwarz will be the 1998 recipient of the Liebig Medal of the German Chemical Society.

Georg Hornung **Detlef Schröder** **Helmut Schwarz** **Christoph A. Schalley**

this method and its application to different fields of chemistry.

Let us first briefly resume the key features of NRMS. In a neutralisation–reionisation experiment [Fig. 1(a)], a mass-selected, fast-moving ion beam is subjected to two sequential collision events with appropriate target gases in gas cells along the flight path. In the first collision, a fraction of the ions is neutralised by a single electron transfer. Then, the remaining ionic species are deflected by applying a high voltage to a deflector electrode, which is located between the two gas cells. Subsequently, the fast moving neutrals are reionised by yet another collision in the second gas cell. Finally, the reionised particles are analysed by standard mass spectrometric means and serve as an indirect probe for the existence of the neutral intermediates. Two particular features of NR mass spectra have attracted considerable attention. (i) The detection of a recovery signal at the *m/z* ratio of the original projectile ions indicates that these ions have survived the whole series of neutralisation and reionisation events. Accordingly, the corresponding neutral counterparts have lifetimes exceeding the time delay between the two electron transfer steps and are typically covering the microsecond regime. (ii) The fragmentation pattern of NR spectra often contains valuable structural information about the connectivities of the neutral species as well as the projectile and survivor ions.

The NR approach, which is complementary to other experimental techniques that are employed for the investigation of isolated neutral molecules, such as matrix isolation or molecular beam spectroscopy, offers three features (i) With the exception of pulsed ionisation methods, the whole repertoire of ionisation methods can be applied for the formation of the precursor ions for NRMS experiments. The ion connectivities can well be identified by collisional activation (CA) experiments. Since ion structures, different from the connectivities of conventional neutral molecules, are often easily accessible, NRMS allows for the generation of unusual neutral species. (ii) In keV collisions, the electron transfer proceeds within *ca.* 10^{-15} s and can, therefore, be regarded as vertical, *i.e.* geometry changes during the neutralisation and reionisation steps are negligible. Accordingly, Franck–Condon factors[14] associated with neutralisation and reionisation dominate the efficiency of the NR process, the internal energy deposited in the neutral and reionised species, as well as the fragmentation pattern (Fig. 2). (iii) Solvent effects and other intermolecular interactions are strictly excluded in the high vacuum existing inside a mass spectrometer.

NR mass spectrometric techniques can be performed in several variants, which contribute significantly to the large body of NR literature.[1–8] (i) Depending on the charges of the projectile and recovery ions, the NR procedure as depicted in Fig. 1(a) can be performed in four variants denoted according to McMahon *et al.*[4] as $^{-}NR^{-}$, $^{-}NR^{+}$, $^{+}NR^{-}$, and $^{+}NR^{+}$. (ii) For structural characterisation or reactivity studies, the survivor ions can be mass selected with the following sector and submitted to collisional activation in the subsequent field-free region provided that its intensity is large enough [NR/CA; Fig. 1(b)].[15] Comparison of the NR/CA mass spectra with conventional CA spectra recorded under the same conditions provides information about the geometric structure of the reionised ions and the purity of the parent ion beam. (iii) Neutrals generated in unimolecular or collision-induced decompositions can be

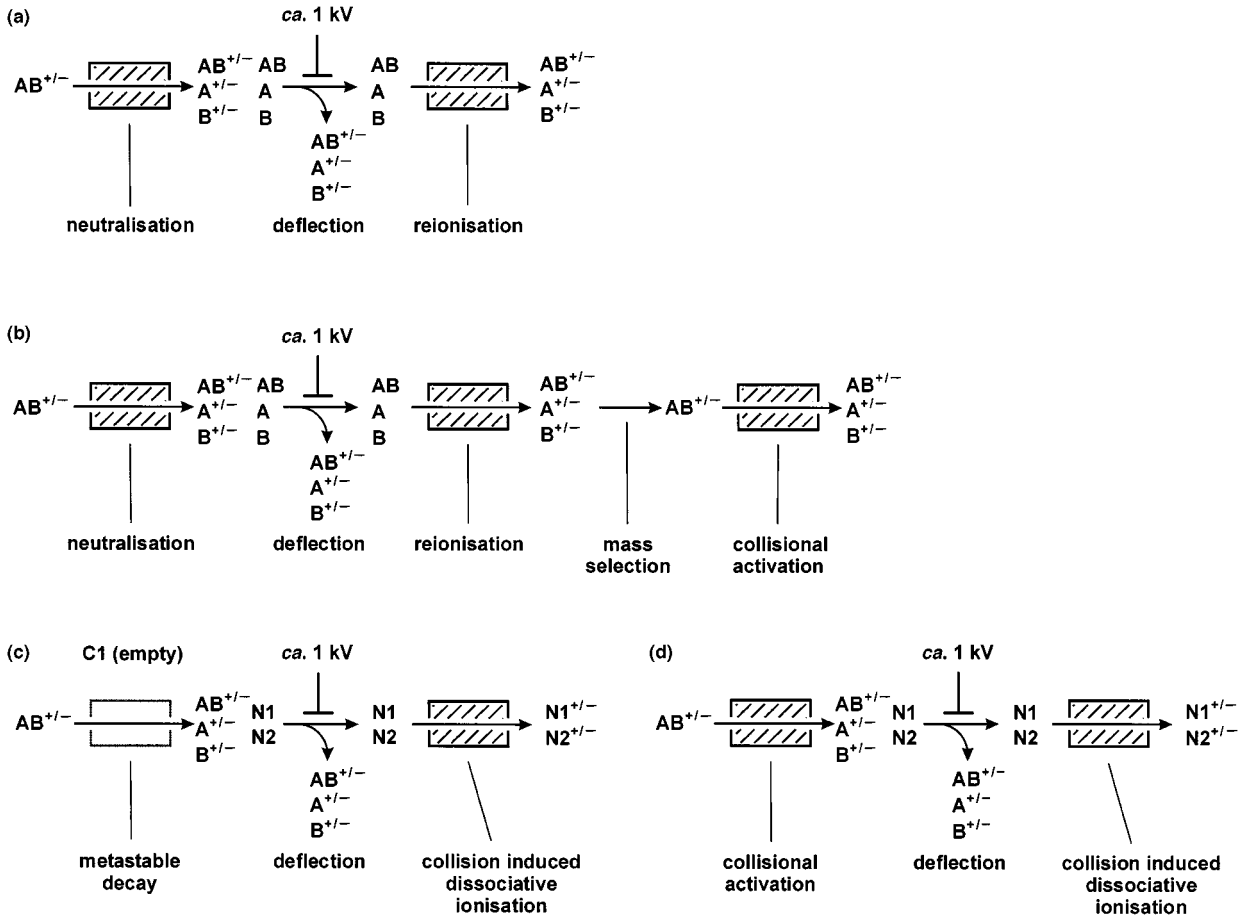

Fig. 1 Typical experimental set-ups for variants of neutalisation-reionisation (NR) experiments: (a) conventional NR procedure with mass selected $AB^{+}/^{-}$, (b) collisional activation of survivor ions $AB^{+}/^{-}$ generated in a NR experiment (NR/CA), (c) collision-induced dissociative ionisation (CIDI) of neutrals N1 and N2 originating from metastable transitions of the parent ions $AB^{+}/^{-}$, and (d) neutral fragment reionisation (N_fR) of neutral N1 and N2 generated by collisional activation of the parent ions $AB^{-}/^{+}$.

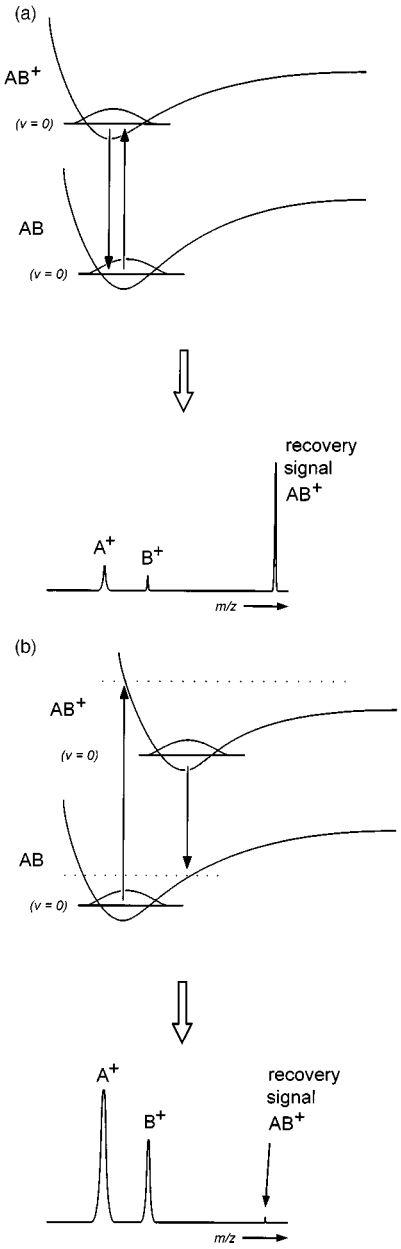

Fig. 2 (a) Schematic $^{+}NR^{+}$ spectrum of AB^{+} being geometrically similar to neutral AB. This results in favourable Franck–Condon factors and hence little fragmentation. (b) Schematic $^{+}NR^{+}$ spectrum of AB^{+} for which the cation and neutral geometries largely differ and thus Franck–Condon factors become unfavourable. AB is formed with a higher internal energy (dotted line), and upon reionisation AB^{+} may be formed rovibrationally excited above the dissociation threshold. Thus, although both AB^{+} and AB are stable species, the recovery signal may be small or even absent and fragmentation prevails.

characterised by collision-induced dissociative ionisation [CIDI; Fig. 1(c)] and neutral fragment reionisation [N_fR; Fig. 1(d)], respectively.[16,17]

Except for a few investigations, up to 1994 the applications of the NR methodology were focussed on the unique capability of probing the existence and structure of unconventional neutral molecules and, as a spin-off to elucidate cation structures for which differentiation between isomers turned out to be difficult by collisional activation. Due to some major obstacles, the question of the neutrals' chemical reactivity, however, has only scarcely been addressed. For example, the unambiguous analysis of the neutrals' reactivity based on the analysis of mass spectra is often difficult to achieve due to a superposition of the fragmentations of the neutral intermediate, the projectiles, and the reionised ions in the NR mass spectra. Further, the microsecond timescale of NR experiments often renders the detection of neutral decompositions difficult due to their low intensities. In addition, most of the methods discussed below require an advanced experimental set-up for an unequivocal detection of the neutrals' fragmentations. Nevertheless, it remains challenging to study the chemical reactivity of transient neutrals produced by NR mass spectrometry, because many of these species have unique electronic or structural features and cannot be generated by other experimental methods. In the past few years, several modifications of the conventional NR technology have been developed in order to extend its capability toward neutral reactivity. Far from giving a comprehensive overview, we will discuss these methods in the following sections in an approximately chronological order together with some instructive examples.

In general, three different approaches can be distinguished. (i) Peak shape analysis may provide information about the kinetic energy releases associated with decomposition reactions of ions and/or neutrals. In favourable cases, the energy releases are different for ions and neutrals which then is reflected in the peak shapes. (ii) Fragmentations of the neutrals species can be induced by collisions with an appropriate target gas or by photoexcitation with a laser beam. This approach does not however monitor the intrinsic, unimolecular reactivity of the transient neutrals. (iii) Variations of the neutrals' lifetimes by different lengths of the flight paths between neutralisation and reionisation allow for an analysis of the unimolecular processes. The advantages and drawbacks of each method will be addressed in the following sections.

2 Early studies

In the early days of NR mass spectrometry, Gellene and Porter[1] derived some information about neutral species from the peak shape of the neutral beam. Upon fragmentation of the hot neutral transients a fraction of the internal energy is released as kinetic energy thus resulting in line broadening of the peak. This information is also contained in the peak shapes of conventional NR mass spectra and composite peaks may indicate superpositions of neutral and ionic decompositions leading to the same products with different kinetic energy releases.

Los *et al.* developed the differential translational spectroscopy[18] which allows the study of the unimolecular decay of neutral molecules generated in a collision of a fast moving ion with a target gas. By this approach the mass ratio of both neutral fragments and the amount of kinetic energy released can be measured. Neutral $CH_3CO^{\bullet}$ radicals, for example, reveal dissociation into $CH_3^{\bullet}$ and CO after randomisation of the internal energy. The measured kinetic energy releases even provide information about the dynamic properties of the reaction in that a model for the conversion of bending motion into fragment translation has been derived.

Neutral $CH_3CO^{\bullet}$ radicals have also been examined by CIDI of $CH_3CO^{\bullet}$ generated unimolecularly from bisacetyl and by NR of CH_3CO^{+} as formed from ionised acetone.[19] In the CIDI mass spectrum, ionised acetyl radical represents the base peak, while the recovery signal is weak in the NR mass spectrum. By peak-shape analysis, it can be shown that $CH_3CO^{\bullet}$ undergoes two fragmentations [eqns. (1) and (2)] when formed by neutralisation of CH_3CO^{+}.

$$CH_3CO^{\bullet} \rightarrow CH_2CO + H^{\bullet} \quad (1)$$

$$CH_3CO^{\bullet} \rightarrow CO + CH_3^{\bullet} \quad (2)$$

These observations were explained by Frank–Condon factor dominated neutralisation of the linear CH_3CO^{+} cation giving rise to excited $CH_3CO^{\bullet}$ radicals which rapidly dissociate. In contrast, unimolecular dissociation of bisacetyl leads to the bent ground state of the $CH_3CO^{\bullet}$ radical which hardly dissociates.

Another approach to probe the neutrals' reactivity was introduced in 1986, when McLafferty and co-workers examined

ylides such as CH_2XH (X = F, Cl, OH, NH_2) and their conventional counterparts CH_3X by NR experiments applying Hg and He as target gases for neutralisation and reionisation, respectively.[20] By varying the helium pressure within the reionisation cell they found significant changes in the NR mass spectra, which were attributed to collision-induced dissociation reactions of the neutral intermediate. For example, in $CH_3Cl^{+\bullet}$ the weakest bond is a C–H bond, while in neutral CH_3Cl the C–Cl bond is cleaved more readily. By increasing the reionisation gas pressure that results in a decrease of transmittance (T) from 90% to 30%, the Cl^+ signal in the NR mass spectrum of CH_3Cl increased dramatically. This has been attributed to dissociation of neutral CH_3Cl into $CH_3^\bullet$ + $Cl^\bullet$ induced by additional collisions before reionisation. In contrast, a drastic increase of the signals for Cl^+ *and* $HCl^{+\bullet}$ was observed for the ylide isomer, CH_2ClH. Unfortunately, this technique[20] suffers from some ambiguities concerning the sequence of collision induced decomposition and reionisation. It is not quite clear whether reionisation comes first, followed by a decay of the reionised ions, or *vice versa*. In short, this method can only be applied to rather small systems, in which distinctly different dissociation channels of neutral and ionic species exist. Thermochemical data or theoretical calculations may then help to decide whether the fragments are due to neutrals or ions. For larger molecules, however, it becomes increasingly more difficult to analyse their reactivity merely on the basis of NR mass spectra obtained with different reionisation gas pressures. Furthermore, thermochemical data are often incomplete for these species and therefore cannot help to decide whether neutral or ionic processes are monitored.

3 Collisional activation of neutral species: the NCR method

In order to avoid these uncertainties, a modified experimental set-up was developed by McLafferty and others[15] which allows for neutralisation, collisional activation of the neutrals, and reionisation (NCR) in three separate and differentially pumped collision cells (Fig. 3). The collision conditions in the second cell can be varied independently with respect to the choice of appropriate gases and transmittances. For collisional activation, helium is most often used, since it reduces the contribution of electron transfer processes. In these experiments, two deflector electrodes are required in front of and behind the second collision cell for separating the neutral beam after neutralisation and deflecting all ions formed in the second cell.

Using the NCR approach, Turecek *et al.* were able to demonstrate that neutral cyclohexa-2,4-dienone[21] **8** (Scheme 2)

8 **9**

Scheme 2

does not readily isomerise to the more stable phenol molecule **9**. Even upon collisional activation of neutral **8** in $^+NCR^+$ experiments, some distinct differences between the $^+NCR^+$ spectra of **8** and **9** remained. The results were interpreted in terms of symmetry-forbidden [1,3]- and [1,7]-sigmatropic hydrogen shifts.

The NR and NCR mass spectra of the $[C_2, H_4, O]^{+\bullet}$ isomers $\mathbf{10}^{+\bullet}$–$\mathbf{16}^{+\bullet}$ have provided a comprehensive set of experimental data which allows for the construction of the neutral, semi-quantitative $[C_2,H_4,O]$ potential-energy surface as depicted in Fig. 4.[22] The three most stable isomers, *i.e.* vinyl alcohol **10**, acetaldehyde **12**, and oxirane **14**, correspond to conventional structures, while the biradicals **13** and **15** and the carbenes **11** and **16** are much higher in energy. NCR experiments were used to determine the extent of isomerisations between these local minima and to derive a qualitative estimate of the relative barrier heights. In this study it was found that **11** as well as **13** are both stable, but upon collisional activation, predominant isomerisation to acetaldehyde **12** was observed. Furthermore, **TS11**/**12** and **TS12**/**13** are predicted to be lower in energy than **TS10**/**11** and **TS13**/**14**, respectively. A path for the direct **10** → **12** rearrangement involving a 1,3-hydrogen shift was not found. Similarly, it could be established that **TS15**/**16** must be higher than the exit channel of lowest energy ($CH_3^\bullet$ + $HCO^\bullet$), because methoxy carbene **16** does not rearrange to any of the other $[C_2, H_4, O]$ isomers. In conclusion, this early example demonstrates the performance of NRMS to examine neutrals including some unusual species such as biradicals and carbenes.

For NCR studies it is quite advantageous to perform a series of experiments at several different gas pressures for collisional activation of the neutral beam. As an example, let us refer to a recent study dealing with the unimolecular decay of methyl hydroperoxide cation radicals, $CH_3OOH^{+\bullet}$.[23] In order to obtain information about the structure and stability of ionised $CH_3OOH^{+\bullet}$, $^+NR^+$ and $^+NCR^+$ experiments (Fig. 5) have been performed, which—besides intense recovery signals—revealed fragments such as $O_2^{+\bullet}$, HO_2^+ and CH_2OOH^+. These structure-indicative fragment ions unambiguously point towards a peroxidic connectivity for the cation as well as its neutral counterpart. In addition, strong support for this structural assignment came from the observation of an O–O bond cleavage of the neutral species. While in neutral CH_3OOH the O–O bond is weak, in the corresponding cation radical the C–O bond is cleaved more readily due to changes in bond strengths. These theoretically predicted features are indeed reflected in the NR and NCR mass spectra which contain fragments indicative of these processes. For example, CH_3^+ and HO_2^+ are generated by C–O bond rupture, while HO^+ and HCO^+ indicate O–O bond cleavage. The latter fragment ion is formed from the quite unstable CH_3O^+ by H_2 loss. Comparing the spectra displayed in Figs. 5(b–d), it becomes obvious (Table 1) that the $CH_3^+ : HO_2^+$ and $HO^+ : HCO^+$ ratios remain approximately constant at 2 : 1 and 1 : 11 irrespective of the helium pressure used for collisional activation of neutral CH_3OOH. In contrast, with decreasing transmittance, the HO^+ and HCO^+ intensities increase relative to those of CH_3^+ and HO_2^+ indicating O–O bond cleavage as a major process at the neutral stage. Thus, the structural assignment of a peroxidic connectivity cannot only be based on characteristic fragments, but also on the observation of the expected reactivity of the proposed neutral.

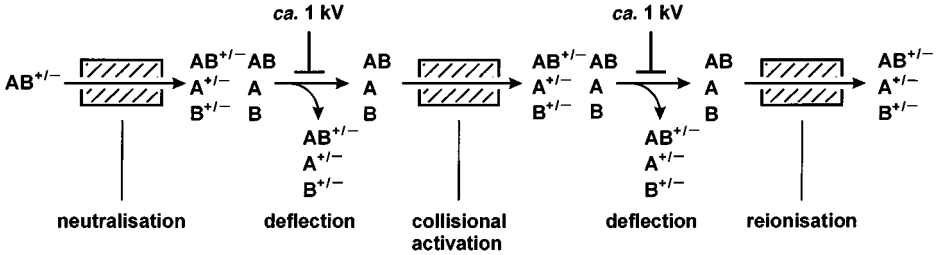

Fig. 3 Set-up of a NCR experiment. After neutralisation and deflection of the remaining ions, the neutral beam is subjected to collisions in a second collision cell and subsequently reionised in the third one. A second deflector electrode ensures that neutrals reionised in the second collision cell are not monitored.

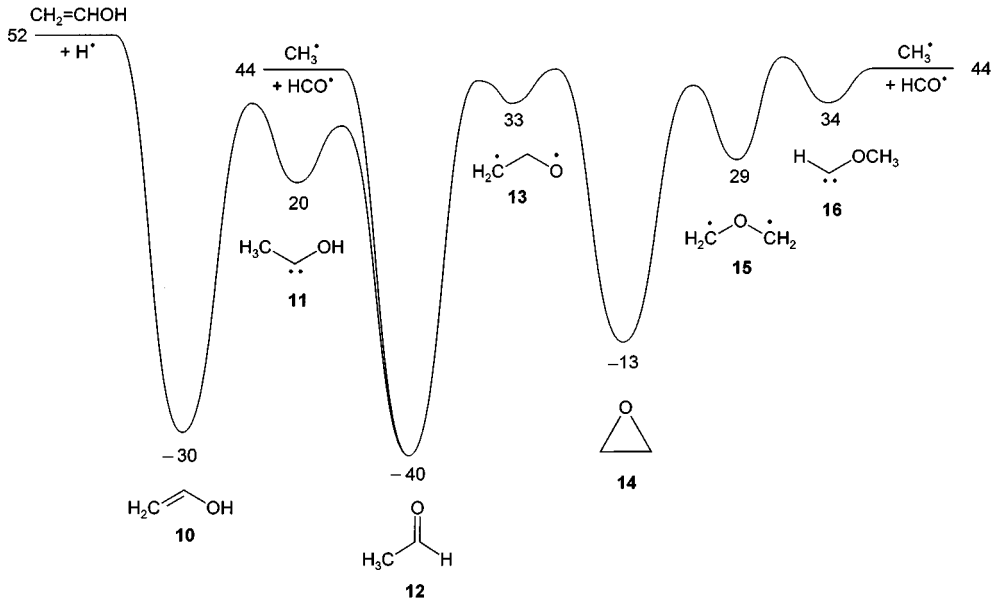

Fig. 4 [C_2,H_4,O] potential-energy surface derived from several NR variants with neutralised $[C_2,H_4,O]^+$ isomers **10**–**16**. Heats of formation (ΔH_f in kcal mol^{-1}) have been taken from ref. 22.

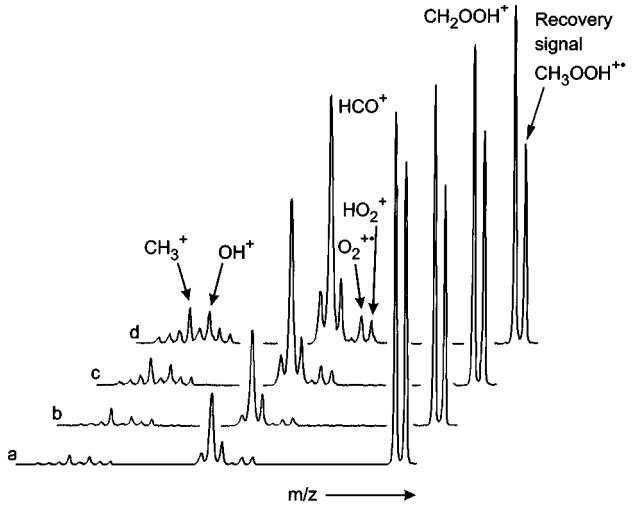

Fig. 5 (a) Conventional (SD)-$^+NR^+$ mass spectrum (Xe, 80% T; O_2 70% T) of $CH_3OOH^{+\bullet}$ using the second and third of three collision cells. (b) (LD)-$^+NR^+$ spectrum (Xe, 80% T; O_2 70% T) with an increased flight path of the neutral intermediates. (c) Same spectrum as (b) applying helium in the second cell for collisional activation of the neutral ($^+NCR^+$; Xe, 80% T; He, 80% T; O_2 70% T). (d) $^+NCR^+$ mass spectrum equal to (c) with increased helium pressure (Xe, 80% T; He, 60% T; O_2 70% T).

Table 1 Ratios of intensities O–O *versus* C–O bond dissociation products in the long distance $^+NR^+$, $^+NCR^+$ (He, 80% T), and $^+NCR^+$ (He, 60% T) mass spectra of $CH_3OOH^{+\bullet}$ [Figs. 5(*b*,*c*,*d*)][a]

Ion pair	LD-NR[b] (100% T)	NCR (80% T)	NCR (60% T)
CH_3^+ : HO_2^+	2.0 : 1.0	2.0 : 1.0	1.0 : 1.0
HO^+ : HCO^+	1.0 : 11.3	1.0 : 11.1	1.0 : 10.2
CH_3^+ : HO^+	2.0 : 1.0	1.4 : 1.0	1.2 : 1.0
HO_2^+ : HO^+	1.0 : 1.0	1.0 : 1.3	1.0 : 1.4
CH_3^+ : HCO^+	1.0 : 5.6	1.0 : 7.1	1.0 : 7.3
HO_2^+ : HCO^+	1.0 : 11.1	1.0 : 13.2	1.0 : 12.5

[a] The conventional $^+NR^+$ spectrum [Fig. 5(a)] is not included in the Table, because the relative intensities may be subject to mass discrimination (see text). [b] Long distance-NR mass spectrum (see Chapter 4).

A drawback of NCR is that collision induced and not unimolecular fragmentations are monitored. While collisional activation is advantageous for a structural characterisation due to direct bond ruptures, it does not necessarily give insight into low-energy pathways which often involve rearrangements. Indeed, a method for the investigation of the decay of metastable neutral species is provided by variation of the flight path and, as a consequence, the lifetimes of the neutrals. A longer flight path is expected to result in increased intensities for those processes which take place at the neutral stage. Ideally speaking, while all collision induced processes occurring during neutralisation and reionisation should be constant in a series of experiments, the unimolecular processes are expected to gain in intensity with increasing lifetime. In the next chapters some aspects of this approach will be outlined.

4 Variation of the neutrals' lifetimes

To a first approximation, the same experimental set-up as used for NCR experiments [Fig. 6(b)] can be applied. Neutralisation in the first collision cell, followed by deflection of all remaining ions with both deflector electrodes and reionisation of the neutral beam in the third cell ('long distance' LD-NR) affords a substantially longer flight path as compared to NR experiments using cells 2 and 3 together with the second deflector only ['short distance' SD-NR, Fig. 6(a)]. Comparison of these spectra allow us to identify the reactions occurring at the neutral stage. However, some limitations should be mentioned. (i) The neutral beam cannot be guided by ion optics as ions can. Thus, a longer flight path may result in larger mass discrimination effects than the shorter one. Direct comparison of SD- and LD-NR mass spectra is, therefore, mostly restricted to ratios of fragments with similar masses. (ii) Often the time range is too short to observe fragmenting neutrals. For example, the SD- and LD-NR mass spectra of the acepentalene system[9] do hardly differ from each other indicating that the neutral does not decompose in the μs timescale. (iii) As the neutralisation step occurs in different collision cells, it may be difficult to ensure that perfectly identical conditions prevail in both experiments.

As a brief example, let us return to methyl hydroperoxide[23] for which Fig. 5 does not only show the NCR experiments, but includes the SD-NR [Fig. 5(a)] and LD-NR (Fig. 5(b)] mass spectra. In good agreement with the NCR results, the ratio of HCO^+ and HO_2^+ fragments changes from the shorter (*ca.* 8 : 1) to the longer (*ca.* 11 : 1) flight path indicating cleavage of the

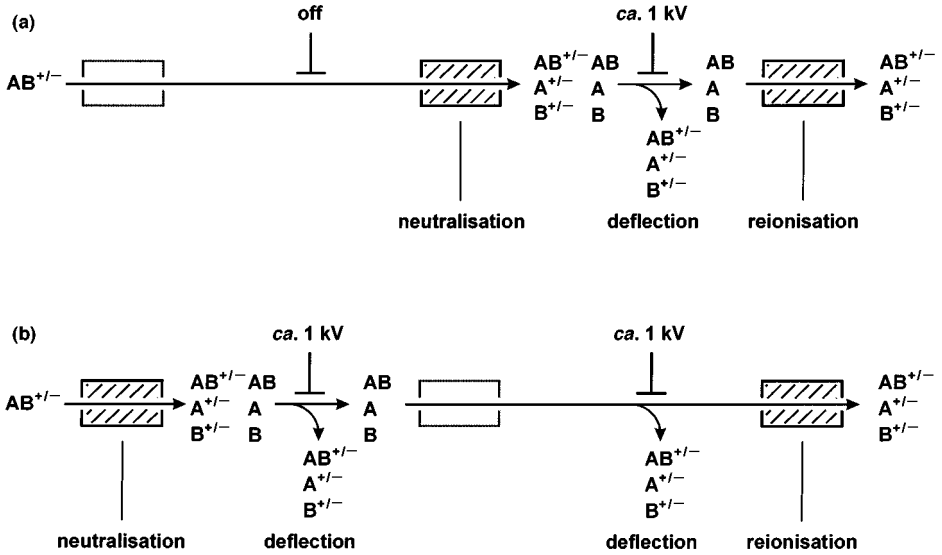

Fig. 6 (a) Short distance (SD) NR experiment. Cell 1 is empty and a conventional NR experiment is performed using cell 2 and 3 together with the second deflector. (b) Long distance (LD) NR experiment. Neutralisation is achieved in cell 1 and reionisation in cell 3, while the second cell is empty and both deflectors are used.

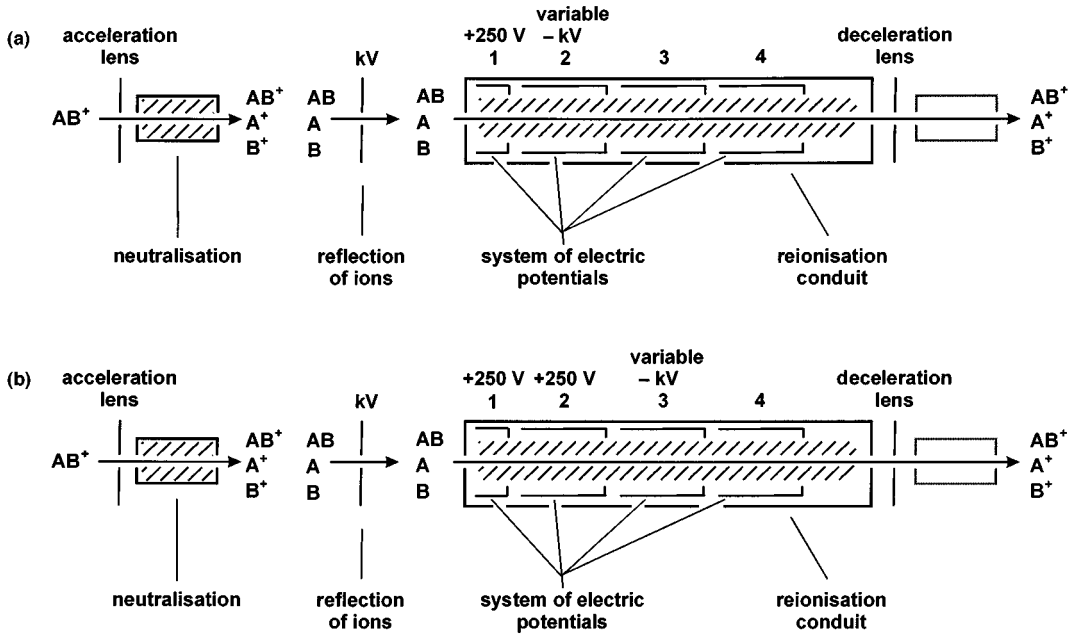

Fig. 7 Instrumentation used for variable-time neutralisation-reionisation experiments with a tandem quadrupole acceleration-deceleration mass spectrometer. After acceleration of the ions, neutralisation occurs in a first collision cell and remaining ions are reflected by an electric potential. Subsequently, reionisation occurs in a 60 cm conduit under single collision conditions. A system of electric potentials and a particular scan mode is used to distinguish reionised species formed in the desired region of the conduit from those generated downstream. (a) Short and (b) long flight paths. For details, see ref. 24.

peroxidic O–O bond as the predominant neutral reaction pathway.

In 1994, Kuhns and Turecek[24] introduced a new technique (Fig. 7) to vary the neutrals' lifetimes in the NR experiments by using a tandem quadrupole acceleration-deceleration mass spectrometer equipped with an advanced collision cell device. After acceleration, the ion beam is neutralised in the first collision cell and the unreacted ions are reflected by an electric potential. The second collision cell consists of a 60 cm flight tube, the conduit, segmented into four regions [Fig. 7(a), 1–4] and equipped with a system of electric potentials. The neutral beam is reionised throughout the whole flight tube. However, by appropriately adjusting the electric potentials, only the ions formed in one of the four segments of the conduit can be monitored. A short neutral flight path is realized in Fig. 7(a). Ions formed in segment 1 floated at +250 V do not have kinetic energies which fit the voltage at the deceleration lens and at the second quadrupole and are not registered. In contrast, ions formed in segment 2 floated at a higher voltage, which is scanned simultaneously with the deceleration lens and the second quadrupole, are detected. By switching from one [Fig. 7(a)] of these regions to the next [Fig. 7(b)], the flight path of the neutrals is increased, while that of the ions becomes shorter in the opposite sense. Only species reionised in segment 3 are monitored now. Comparison of the spectra obtained in this manner allows us to distinguish between neutral and ion fragmentations, because those of the neutrals become more intense, while ion decay decreases in intensity due to the shorter ion flight path. It is important to note that the collision gas is admitted uniformly to the flight tube at a pressure which guarantees single collision conditions (*ca.* 90% T). This ensures comparable reionisation conditions at each of the subunits of the conduit and avoids the problems connected with switching between different collision cells for neutralisation as described

above for long and short distance NR experiments. Furthermore, under these conditions *ca.* 95% of the reionised particles undergo only one collision which leads to reionisation. Thus, unimolecular decompositions of the neutrals can be monitored, while collision induced decompositions only contribute to a very minor extent.

A kinetic analysis of ion and neutral fragmentations is possible using the variable-time NR technique provided that the relative reionisation cross sections are known or can be measured. This procedure yields phenomenological dissociation rate constants k_n for neutral and k_i for ionic species in the range of 10^4–10^6 s^{-1}.[24] Much faster or slower fragmentations of the neutrals cannot be resolved within the 100 ns–5 μs timescale of the variable-time NR experiment. As an example, let us refer to the measurement of the rate constant k_n for the decay of a beam of methyl iodide, CH_3I, which demonstrated that the resonant electron transfer using CH_3I for neutralisation yields neutral methyl iodide with only modest excitation energy. In contrast, off-resonance neutralisation of the $CH_3I^{+\bullet}$ beam with other target gases gave rise to higher rate constants, which were rationalised by invoking initial formation of Rydberg states.

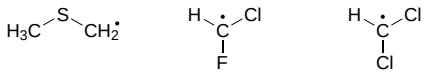

17$^\bullet$ **18**$^\bullet$ **19**$^\bullet$

Some atmospherically important radicals, *i.e.* $CH_3SCH_2^\bullet$, **17**$^\bullet$, $CHClF^\bullet$, **18**$^\bullet$, and $CHCl_2^\bullet$, **19**$^\bullet$, have been studied by this technique.[25] For example, the oxidation of dimethyl sulfide has been proposed to involve the reaction of HO$^\bullet$ radicals with dimethyl sulfide, and the methylthiomethyl radical **17**$^\bullet$ is believed to be an important intermediate. In line with results obtained from NR and NCR experiments, variable-time NR experiments not only suggest **17**$^\bullet$ to be a stable species, but also demonstrate that neutral **17**$^\bullet$ decomposes unimolecularly *via* methyl loss. As far as reaction kinetics are concerned, the fragmentation of reionised **17**$^\bullet$ proceeds, however, at a higher rate constant as that of neutral **17**$^\bullet$. Similarly, **18**$^\bullet$ and **19**$^\bullet$ have been reported to dissociate into CHF + Cl$^\bullet$ and CHCl + Cl$^\bullet$, respectively; both radicals may serve as sources for chlorine atoms relevant for ozone depletion in the upper atmosphere.

Variable-time NR mass spectrometry has also been applied for investigations of fundamental issues in organic chemistry, *e.g.* the protonation sites of pyridine.[26] It is quite clear that the nitrogen atom represents the most basic position of pyridine, followed by C(3), C(2) and C(4) with decreasing proton affinities. Combining isotopic labelling with neutralisation-reionisation experiments allows us to distinguish between N- and C-protonation. The basic idea is depicted in Scheme 3. If the

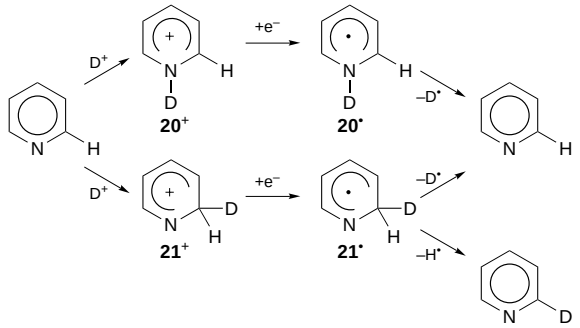

Scheme 3

nitrogen atom in pyridine is deuteriated and cation **20**$^+$ subsequently neutralised, exclusive loss of a deuterium atom from neutral **20**$^\bullet$ is expected. In contrast, C-protonation may yield hydrogen and deuterium losses from intermediate **21**$^\bullet$. These experiments have, of course, to be cross-checked with protonated [$^2H_5$]pyridine in order to account for kinetic isotope effects. Experimentally, exclusive N-protonation was found for weak Brønsted acids such as $CH_3NH_3^+$, NH_4^+, *tert*-$C_4H_9^+$ and H_3O^+, while a small fraction of C-protonated pyridine **21**$^+$ was formed in the reaction of pyridine with CH_5^+.

Another interesting feature of the NR mass spectra of protonated pyridines is the observation of recovery signals which demonstrate the existence of hypervalent pyridinium radicals to be stable species. Earlier, the groups of Porter[1] and others[27,28] provided evidence that a variety of hypervalent species such as $H_3^\bullet$, $ND_4^\bullet$, and $D_3O^\bullet$ do exist in the gas phase. This field of NR mass spectrometry has recently been revisited by the variable-time NR and NCR techniques. For example, several hypervalent ammonium radicals[29] with different substitution patterns and tetracoordinated oxygenated phosphorus radicals[30] have been investigated. For alkyl substituted **22**$^\bullet$, **23**$^\bullet$

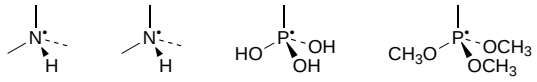

22$^\bullet$ **23**$^\bullet$ **24**$^\bullet$ **25**$^\bullet$

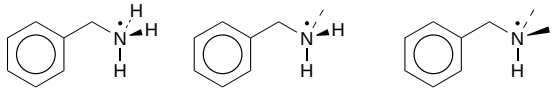

26$^\bullet$ **27**$^\bullet$ **28**$^\bullet$

and **26**$^\bullet$–**28**$^\bullet$ homolytic cleavages of N–H, N–CH_3, or N–CH_2Ph bonds prevail thus giving rise to the corresponding neutral amines. While the transient existence of these radicals has been proven by the observation of recovery signals for deuterated isotopologues of **22** and **23**, no recovery signals were found in the $^+NR^+$ mass spectra of neither **26**$^+$–**28**$^+$, nor their deuterated analogues.

Similarly, for the tetrahydroxy phosphonium radical **24** no recovery signal was detected.[30] Theory, however, predicts **24** as a stable species, for which the loss of H$^\bullet$ (ΔH_r = −7 kcal mol^{-1}) and water (ΔH_r = −2 kcal mol^{-1}) represent thermodynamically favourable fragmentation channels. These are indeed observed in the NR and NCR experiments carried out with $P(OH)_4^+$ cations. In contrast, for the cationic $P(OH)_4^+$ precursor these two reaction pathways are endothermic by *ca.* 120 and 69 kcal mol^{-1}, respectively. Thus, it is unlikely that the hydrogen atom and water losses occur at the cationic stage. Similarly, **25** reacts *via* losses of H$^\bullet$ and $CH_3^\bullet$ yielding $(CH_3O)_3PO$ and $(CH_3O)_2(HO)PO$ as products. In contrast to **24**, for **25** also losses of HO$^\bullet$ and $CH_3O^\bullet$ radicals are observed, thus producing $(CH_3O)_3P$ and $(CH_3O)_2P(OH)$ as neutral products.

Most recently, variable-time NR experiments were performed with neutral $H_3S^\bullet$ radicals and its D and ^{34}S labeled isotopologues.[31] These experiments not only demonstrated that these exist as transient neutrals, but also unraveled their reactivity. Hydrogen atom losses dominate, which are affected by a normal kinetic isotope effect. As observed earlier[1,7] for other hypervalent radicals, neutralisation of vibrationally excited precursor ions leads to an increase of the recovery signal intensity. This indicates that hot precursor ions, due to more favourable Franck–Condon factors, have a higher probability of being neutralised into stable states of the hypervalent radicals.

5 Photoexcitation of transient neutrals

The metastability of hypervalent radicals due to the presence of bound excited states has been under intense discussion, not the least because of some inconsistencies in the interpretation of the data. While theory in some cases predicted unstable or very weakly bound ground states, the experiments showed hypervalent radicals to exist.[1] In order to probe further this aspect, irradiation of the neutral species with photons of wavelengths suitable for the ionisation of metastable excited states, but not the ground states, seems a promising strategy, and an appropriate experiment was designed by the group of Turecek.[32]

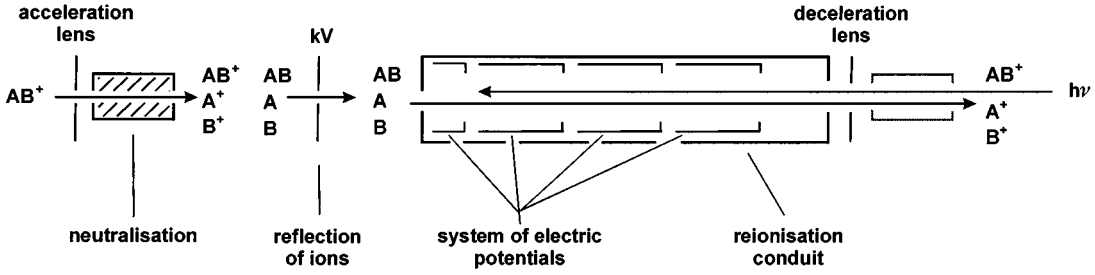

Fig. 8 Instrumentation for laser photoionisation experiments: an Ar laser (488 and 514.5 nm) is directed antiparallel to the flight axis of the neutral particle beam. The neutrals are allowed to interact with the photons throughout the whole length of the conduit (60 cm).

They equipped their tandem quadrupole acceleration-deceleration mass spectrometer shown in Fig. 7 with a laser that is directed antiparallel to the axis of the particle beam (Fig. 8).

Upon photolysis of metastable $ND_4^{\bullet}$ radicals with photons in the range of 2.41–2.54 eV, only a very minor fraction of ND_4^+ is formed.[32] As the ground state bears an ionisation energy of 4.6 eV, these ions cannot be generated from ground state $ND_4^{\bullet}$. Rather, a small amount of excited $ND_4^{\bullet}$ was generated in the neutralisation step. In contrast, the signals corresponding to ND_3 and $ND_2^{\bullet}$ are much more intense owing to photodissociation of ground state $ND_4^{\bullet}$ and subsequent reionisation of the ND_3 and $ND_2^{\bullet}$ fragments. This rationale is in agreement with the potential energy diagram depicted in Fig. 9 for $NH_4^{\bullet}$. The

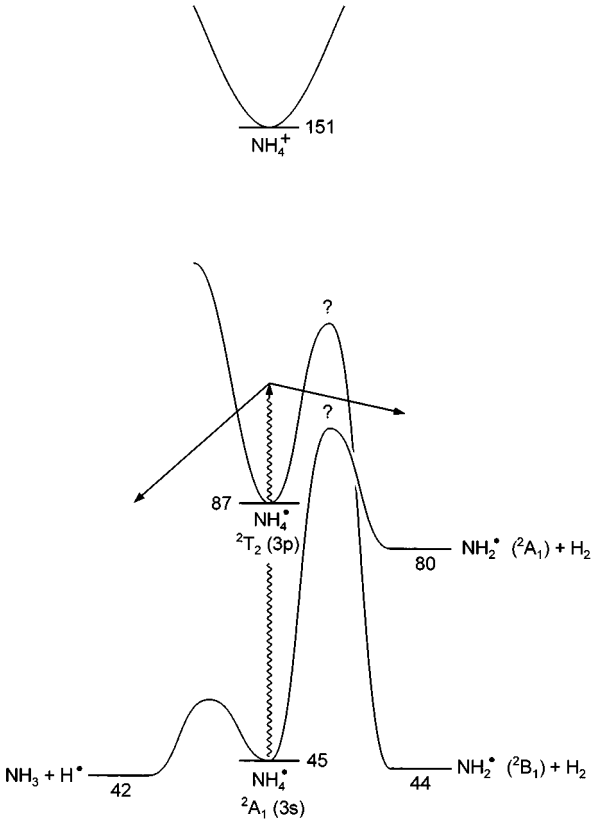

Fig. 9 Potential-energy diagram (kcal mol^{-1}) for $NH_4^{\bullet}$.

$^2A_1$ ground state is prevented by a barrier of *ca.* 0.41 eV (*ca.* 9.5 kcal mol^{-1}) from dissociation into $NH_3 + H^{\bullet}$. The barrier for the loss of H_2 with concomitant formation of $NH_2^{\bullet}$ in its $^2A_1$ state is even higher, but still below the excitation limit given by the photon energy. In contrast to the ground state, the excited $^2T_2$ state is kinetically much more stabilised. However, dipole-allowed transitions to lower states are possible, and the $^2T_2 \rightarrow {}^2A_1$ transition may explain that only a minor fraction of excited $ND_4^{\bullet}$ survived the time delay between neutralisation and photoionisation.

A distinctly different picture is found for dimethyldeuteriooxonium radicals, $(CH_3)_2OD^{\bullet}$ **29**$^{\bullet}$.[32] This species is found experimentally to be metastable against the thermodynamically favourable dissociations into either $(CH_3)_2O + D^{\bullet}$ or $CH_3OD + CH_3^{\bullet}$, and metastable **29**$^{\bullet}$ is easily photoionised by 2.41–2.54 eV photons. Theory predicts the $^2A'$ ground state of **29**$^{\bullet}$ to be repulsive with respect to dissociation of the O–H(D) bond (Fig. 10). However, the excited $^2A''$ electromer, which is characterised as a 3p Rydberg state, is expected to be metastable. Its vertical ionisation energy amounts to 2.22 eV, which matches the range of the photon energies.

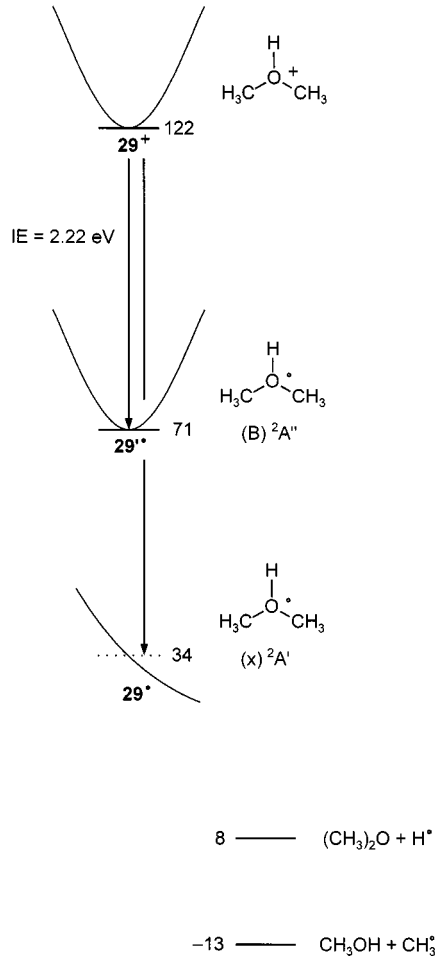

Fig. 10 Potential-energy diagram (kcal mol^{-1}) for ground and excited states of $(CH_3)_2OH^{\bullet}$ **29**$^{\bullet}$.

These few examples may suffice to demonstrate the performance of a combination of NR experiments with photochemistry for the examination of metastable excited states. It should be noted, however, that one has to account for multi-photon ionization when using this technique. For the detection of high Rydberg states, which are transparent for the Ar laser beam, field ionisation provides an attractive alternative.[3] Thus, the

possibility to perform photoionisation or photodissociation experiments of transient neutrals helps to bridge the gap between ground and Rydberg state chemistry. Application of this method to larger systems may be of quite some interest for future work.

6 Neutral and ion decomposition difference (NIDD) mass spectrometry

In the previous sections, we have described how the unimolecular decay of neutrals, generated by neutralisation-reionisation mass spectrometric experiments can be probed by several techniques. However, these methods require rather special experimental set-ups, which are not common to most of the laboratories concerned with the generation and investigation of elusive neutrals. In this section, a new approach coined 'Neutral and Ion Decomposition Difference' mass spectrometry (NIDD-MS)[33,34] will be described, which can be performed with a conventional NR set-up. Its scope will be demonstrated by applying it to systems as different as the formate anion, peroxide cation radicals, the $^{\bullet}CH_2COO^-$ distonic anion, and alkoxy radicals.

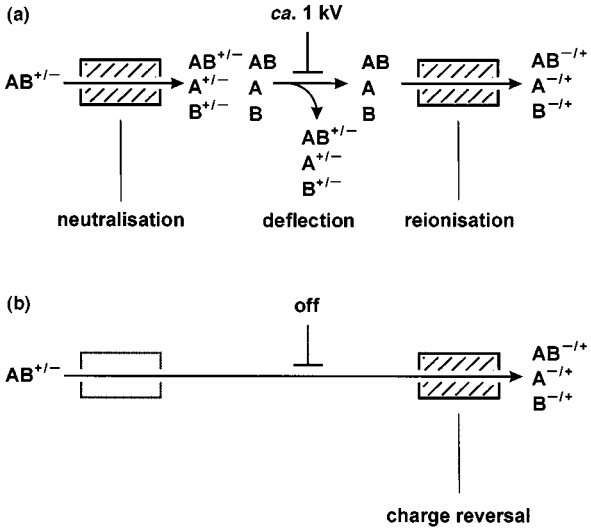

Fig. 11 (a) Conventional NR experiment with charge inversion of the ion beam ($^-NR^+$ or $^+NR^-$, respectively). (b) Charge reversal experiment ($^-CR^+$ or $^+CR^-$).

Recently, the femtosecond dynamics for the formation of three membered Ag_3 rings from its linear form have been studied with a related method.[35] The Negative ion–Neutral atom–Positive Ion (NeNePo) charge reversal spectroscopy relies on the photon-induced, vertical neutralisation of an anion, *e.g.* linear Ag_3^-. This structure represents a transition structure on the neutral potential-energy surface. The ring closure reaction can be monitored by a time-delayed second laser pulse for cationisation of the neutral.

In contrast, the NIDD approach uses collisions instead of laser pulses for neutralisation and reionisation. Here, variation of the lifetimes of the neutral species is achieved by comparing conventional $^-NR^+$ or $^+NR^-$ mass spectra with the corresponding charge reversal[36] mass spectra ($^-CR^+$ or $^+CR^-$, respectively, see Fig. 11). While the NR procedure necessarily requires two separate collision events, and intermediate deflection of the unreacted ions, charge inversion in CR experiments is afforded in a single collision by a two-electron transfer. Ideally speaking, the CR signals are due to ionic fragmentations, whereas in the NR spectra dissociations of ionic and neutral processes are superimposed. Normalisation[33,34] of the spectra to the sum of all fragments followed by subtraction of the CR from the NR intensities [eqn. (3)] results in NIDD spectra, in which processes due to the fragmentations of neutrals have positive intensities, while ionic contributions show up as negative peaks, thus providing firm criteria for the identification of neutral and ionic processes.

$$I_i(NIDD) = [I_i(NR)/\Sigma_i I_i(NR)] - [I_3(CR)/\Sigma_i I_i(CR)] \quad (3)$$

The NIDD method has the major advantage that it uses a standard NR set-up. Thus, both experiments can be conducted rather quickly one following the other, so that ion source conditions and ion focus parameters can be kept constant during the measurements. As will be shown below, NIDD is applicable to the reactivity of open- and closed-shell neutrals and also to both directions of charge inversion.

As a first example, let us discuss the $[C,H,O_2]^{\bullet}$ system in some detail including the results of a theoretical study of the respective potential-energy surfaces.[33,34] The two ionic precursors used are typical organic ions, namely, the formate ion $HCOO^-$ **30**$^-$ and the hydroxyacylium ion $HOCO^+$ **31**$^+$, *viz.* protonated carbon dioxide. The $^-NR^+$ and $^-CR^+$ spectra of formate ion **30**$^-$ [Fig. 12(a,b)] are fairly different from each other. The signals for the recovery ion and the HCO^+ fragment are barely visible in the $^-NR^+$ spectrum, but quite intense in the $^-CR^+$ experiment. Due to these pronounced differences, in the $^-NIDD^+$ spectrum [Fig. 12(c)] $CO_2^{+\bullet}$ is the dominant feature on the positive scale. Thus, we conclude that the formoxyl radical $HCOO^{\bullet}$ formed upon electron detachment from $HCOO^+$ dissociates to a large amount by loosing a hydrogen atom, *i.e.* $HCOO \rightarrow CO_2 + H^{\bullet}$, while the HCO^+ fragment arises from the cationic surface. Interestingly, in the spectra of $DCOO^-$ **30a**$^-$ [Fig. 12(d,e)] the recovery signals and also the DCO^+ fragments are much more intense, thus pointing to a sizeable kinetic isotope effect on the stability of the transient formoxyl radical formed upon neutralisation. In contrast, the loss of an oxygen atom to yield HCO^+ or DCO^+, respectively, is not subject to isotope effects. The experimental results are fully confirmed by the potential-energy surfaces of $[C,H,O_2]^+/^{\bullet}/^-$ systems calculated at the Becke3LYP/ 6-311++G(d,p) level of theory (Fig. 13). The barrier for the hydrogen atom loss from $HCO_2^{\bullet}$ (**TS 30**$^{\bullet}$) is expected to be small. Reionisation of the neutral as well as charge inversion of the anion does most likely not involve the singlet HCO_2^+ cation, but rather the triplet analogue, which is calculated to be formed in the $^-CR^+$ experiment with only a negligible amount of excitation energy due to similar geometries. This accounts for the more abundant survivor ion current observed in the $^-CR^+$ experiment. From triplet HCO_2^+ the O-atom loss corresponds to the most favourable exit channel in line with the experiment. Unfortunately, the $^+NR^-$ and $^+CR^-$ mass spectra of protonated carbon dioxide $HOCO^+$ are quite similar and, therefore, cannot be analysed with the NIDD scheme, because in this case the absolute signals in the $^+NIDD^-$ spectrum vanish within experimental error.

As mentioned above, the ionised methyl hydroperoxide bears an intact peroxide connectivity,[23] and the same holds true for the neutral species (see above). Indeed, the $^+NIDD^-$ mass spectrum of $CH_3OOH^{+\bullet}$ (Fig. 14) shows positive signals for the HO^- and CH_3O^- fragments due to O–O bond cleavage in neutral methyl hydroperoxide. In contrast, all fragments due to C–O or H–O bond ruptures are negative, indicating their ionic origin. Overall the reactivity of peroxides[33,37] generated by collisional neutralisation of the cations follows expectation and demonstrates the applicability of $^+NIDD^-$ for the examination of the reactivities of transient closed-shell neutrals in the gas phase.

Similarly, the $^+NIDD^-$ mass spectrum of ionised hydrogen peroxide [Fig. 15(c)] shows an intense positive peak for the formation of $HO^{\bullet}$ radicals, again indicating O–O bond cleavage in agreement with the conventional HOOH connectivity. However, the $^+NR^-$ and $^+CR^-$ mass spectra [Fig. 15(a,b)] of $[H_2,O_2]^{+\bullet}$ show a distinct recovery signal which was not observed for the methyl substituted homologues. By detailed experimental and theoretical investigation including $[H,D,O_2]$ and $[D_2,O_2]$ the recovery signal was shown to be due to the long sought after singlet water oxide molecule H_2OO as transient

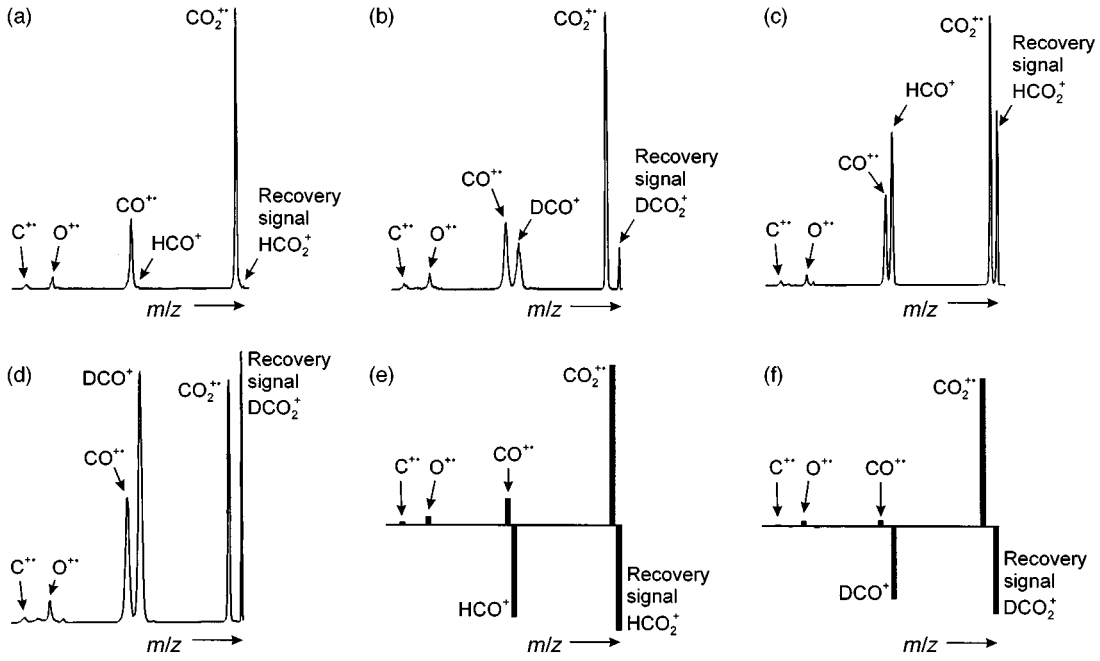

Fig. 12 (a) $^{-}NR^{+}$ mass spectrum (O_2, 80% T; O_2, 80% T), (b) $^{-}CR^{+}$ mass spectrum (O_2, 80% T), and (c) $^{-}NIDD^{+}$ spectrum of formate ion $HCOO^{-}$ **30**$^{-}$ generated by chemical ionisation of formic acid with N_2O as reagent gas. (d)–(f) Analogous spectra for the deuteriated ion $DCOO^{-}$ **30a**$^{-}$.

neutral.[38] Thus, in line with other experiments such as NR/CA, NCR, SD-/LD-NR, it was demonstrated that the neutral beam contains a small amount of the H_2OO isomer within an excess of HOOH molecules. Nevertheless, neutral water oxide could be identified by its ability to form stable anions. The calculated potential-energy surface of neutral $[H_2,O_2]$ (Fig. 16) reveals that the bulk generation of water oxide is not straightforward at all and only sophisticated techniques like NR mass spectrometry can be used to probe its existence at a molecular level. Thus, this example demonstrates once more the enormous potential of the NR technique for the generation of highly reactive and elusive neutrals, which are difficult to produce and detect by any other spectroscopic means. Mass spectrometric means are particularly favourable for the identification of neutral water oxide, since it relies on the $HOOH^{+\bullet} \rightarrow H_2OO^{+\bullet}$ isomerisation of a small amount of the ionised hydrogen peroxide precursors, from which vertical ionisation into the two neutral minima is possible.

One of the most interesting classes of compounds in gas-phase chemistry are the distonic ions, *i.e.* open-shell ions in which radical and charge centres are spatially separated. While these ions can exhibit rather unusual geometric structures, they are in fact quite often thermochemically or kinetically more stable than the conventional ionic counterparts, *e.g.* the $^{\bullet}CH_2OH_2^{+}/CH_3OH^{+\bullet}$ couple. Distonic ions attract on-going attention and the same should apply for the corresponding neutrals because, unless rearrangements occur, these should be formed as ylides from α-distonic ions or as biradicals from β- or higher distonic ions. As a representative for a negatively charged β-distonic ion let us discuss the acetoxy anion $^{\bullet}CH_2COO^{-}$ **32**$^{+\bullet}$.[39] The $^{-}NIDD^{+}$ spectrum (Fig. 17) shows significant positive signals for the $CO_2^{+\bullet}$, $CH_2O^{+\bullet}$, and $CO^{+\bullet}$ fragments which can be interpreted in terms of Scheme 6. Electron detachment from $^{\bullet}CH_2COO^{-}$ leads to the corresponding diradical **32**, either in singlet or triplet states. The neutral triplet then dissociates in the μs timescale into $^3CH_2$ and CO_2 which are subsequently reionised. The singlet, however, can cyclise to α-aceto lactone **33** which gives rise to the $CH_2O^{+\bullet}$ and $CO^{+\bullet}$ fragments, *i.e.* either the excess energy gained in recombination leads to dissociation at the neutral stage followed by reionisation of the neutrals or these fragments are formed upon reionisation of **33**, but not **32**. Recent results from our laboratory show that oxyallyl anion radicals, $^{\bullet}CH_2C(O)CH_2^{-}$, give rise to positive CO and C_2H_4 signals in the $^{-}NIDD^{+}$ spectrum. This indicates that ring closure occurs analogously at the neutral stage. Thus, $^{-}NIDD^{+}$ of radical anions is particularly suitable to examine biradicals which are rather difficult to produce by other means. One particular feature may need further comment: according to Scheme 4, the $CH_2^{+\bullet}$ fragment is

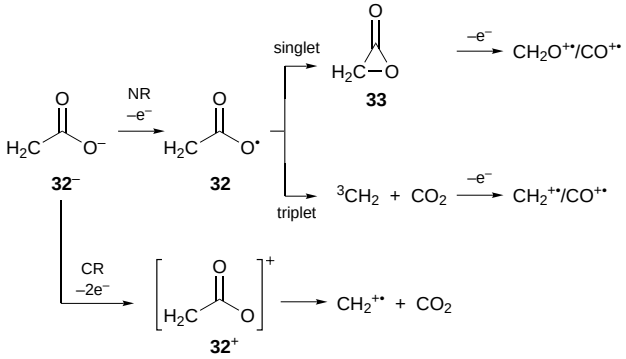

Scheme 4

due to fragmentation of neutral **32** and should thus appear on the positive part of the $^{-}NIDD^{+}$ spectrum, yet it gives rise to a negative signal. According to the NIDD scheme, $CH_2^{+\bullet}$ therefore originates from ionic species, and a facile rationalisation is the direct C–C bond cleavage of the transient $^{\bullet}CH_2COO^{+}$ cation formed upon charge inversion in which the methylene fragment is more likely to be charged, because the ionisation energies of CH_2 (10.4 eV) and CO_2 (13.8 eV) largely differ. Hence, the negative signal for $CH_2^{+\bullet}$ is not in contradiction with the NIDD scheme, because more $CH_2^{+\bullet}$ is formed by direct dissociation of the cations in the $^{-}CR^{+}$ experiment than by reionisation of the methylene fragment in the $^{-}NR^{+}$ process. This and similar compensation effects must, however, be accounted for in the interpretation of NIDD spectra.

As a final example, the gas-phase reactions of neutral alkoxy radicals generated by neutralisation of alkoxide ions will be discussed.[40] Alkoxy radicals have been chosen, because in condensed matter their reactivity is well understood, and they may serve as suitable test systems for the performance of NIDD. Alkoxy radicals with short and/or branched hydrocarbon chains, *e.g.* methoxy, ethoxy, isopropoxy, or *tert*-butoxy radicals,

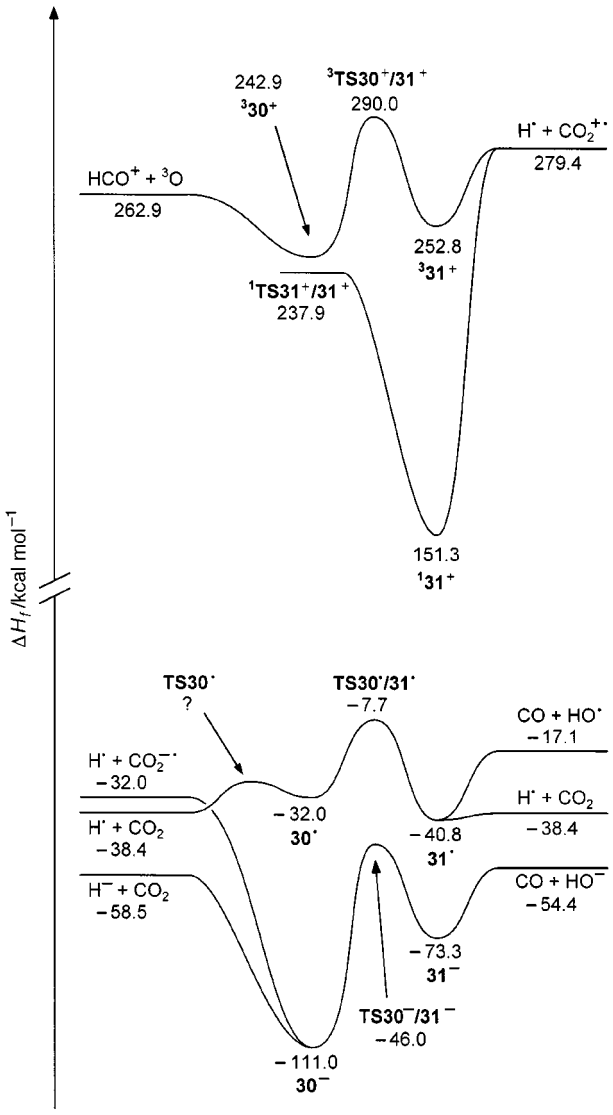

Fig. 13 Potential-energy surfaces of $[C,H,O_2]^{+}/^{\bullet}/^{-}$ species calculated at the Becke3LYP/6-311++G(d,p) level of theory.

undergo α-cleavages [eqns. (4–9)] which give rise to the losses of H$^{\bullet}$ and $CH_3^{\bullet}$ respectively. The intensity ratios observed for C–H and C–C bond cleavage products for ethoxy and isopropoxy radicals are consistent with thermochemistry, with the least endothermic process being favoured in the NIDD spectra.[40]

$$CH_3O^{\bullet} \rightarrow CH_2O + H^{\bullet} \quad (4)$$

$$CH_3CH_2O^{\bullet} \rightarrow CH_3CHO + H^{\bullet} \quad (5)$$

$$CH_3CH_2O^{\bullet} \rightarrow CH_2O + CH_3^{\bullet} \quad (6)$$

$$(CH_3)_2CHO^{\bullet} \rightarrow (CH_3)_2O + H^{\bullet} \quad (7)$$

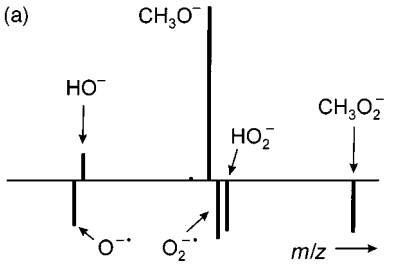

Fig. 14 $^{+}NIDD^{-}$ mass spectrum of methyl hydroperoxide generated by electron ionisation.

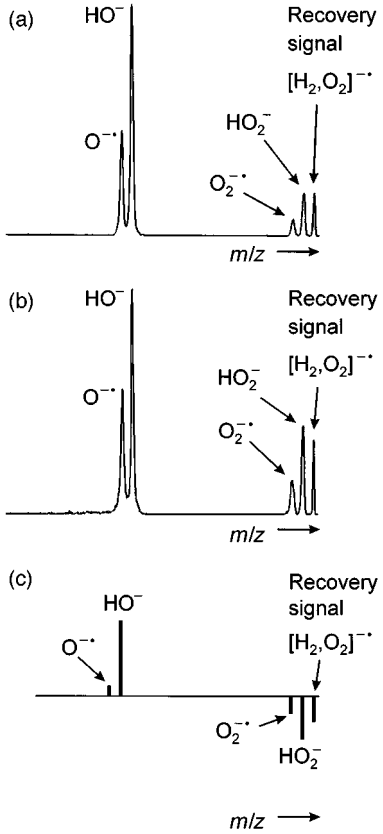

Fig. 15 (a) $^{+}NR^{-}$ mass spectrum (Xe, 80% T; benzene, 70% T), (b) $^{+}CR^{-}$ mass spectrum (benzene, 70% T), and (c) $^{+}NIDD^{-}$ spectrum of hydrogen peroxide cation radicals generated by electron ionisation of H_2O_2.

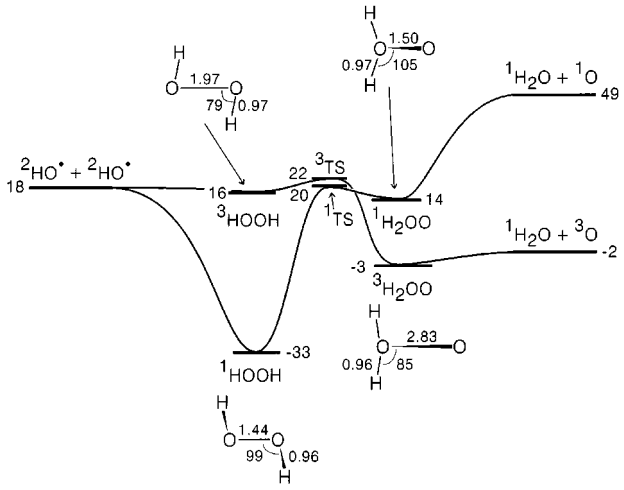

Fig. 16 Potential-energy surfaces of neutral singlet and triplet $[H_2,O_2]$. Heats of formation are given in kcal mol^{-1}.

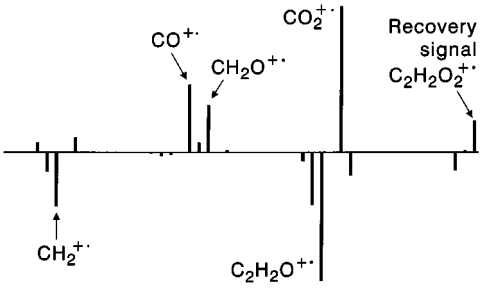

Fig. 17 $^{-}NIDD^{+}$ mass spectrum of $^{\bullet}CH_2COO^{-}$ distonic anion **32**$^{-\bullet}$.

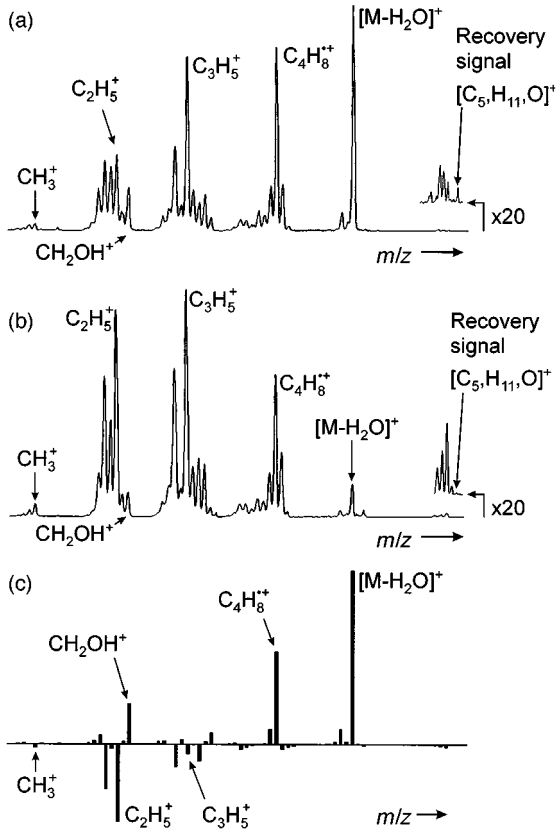

Fig. 18 (a) $^{-}NR^{+}$ mass spectrum (O_2, 80% T; O_2, 80% T), (b) $^{-}CR^{+}$ mass spectrum (O_2, 80% T), and (c) $^{-}NIDD^{+}$ spectrum of pentanolate ions **34**$^{-}$ generated by negative ion chemical ionisation of *n*-pentan-1-ol with N_2O.

$$(CH_3)_2CHO^{\bullet} \rightarrow CH_3CHO + CH_3^{\bullet} \quad (8)$$

$$(CH_3)_3CO^{\bullet} \rightarrow (CH_3)_2O + CH_3^{\bullet} \quad (9)$$

Alkoxy radicals with longer side-chains exhibit remarkably different reactivities. Thus, 1,5-hydrogen migrations become feasible and indeed Barton-type rearrangements are observed. The pentyloxy radical **34**$^{\bullet}$ may serve as an example.[40] While the $^{-}NR^{+}$ and $^{-}CR^{+}$ spectra of **34**$^{-}$ [Fig. 18(a,b)] are rather complicated and difficult to analyse, the $^{-}NIDD^{+}$ mass spectrum of pentoxide ions **34**$^{-}$ [Fig. 18(c)] reveals only three distinct signals on the positive scale corresponding to CH_2OH^{+}, its $C_4H_8^{+\bullet}$ counterpart and the loss of water indicating a hydrogen migration from the alkyl chain to the oxygen centered radical. The $^{-}NIDD^{+}$ mass spectra of deuterium labeled pentoxide ions revealed the occurrence of a clean 1,5-H shift,[40] suggesting the mechanism proposed in Scheme 5, which

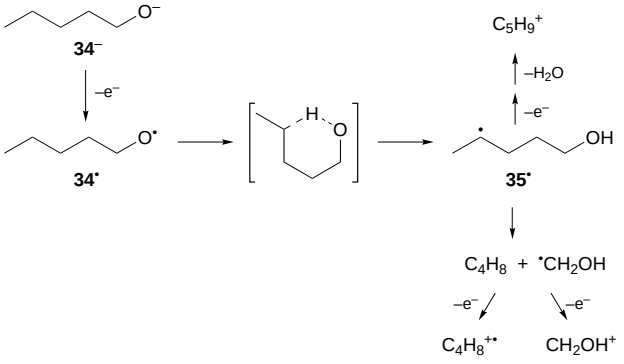

Scheme 5

involves a six-membered transition structure for hydrogen migration with **35**$^{\bullet}$ being the central intermediate from which, upon reionisation, two reaction pathways lead to either the formation of CH_2OH^{+} and $C_4H_8^{+\bullet}$ or to the water loss.

Appropriate substitution of the hydrocarbon backbone even permits us to examine the stereochemical features of the 1,5-hydrogen migration in transient alkoxy radicals. To this end, a methyl group at the C(3) position of a pentyloxy radical was introduced as a stereochemical marker. The stereoselectivity of the hydrogen migration can be monitored using the diastereospecifically labeled [4-^{2}H]-3-methylpentyloxy radicals **36a**$^{\bullet}$ and **36b**$^{\bullet}$ (Scheme 6). The $^{-}NIDD^{+}$ spectra of the

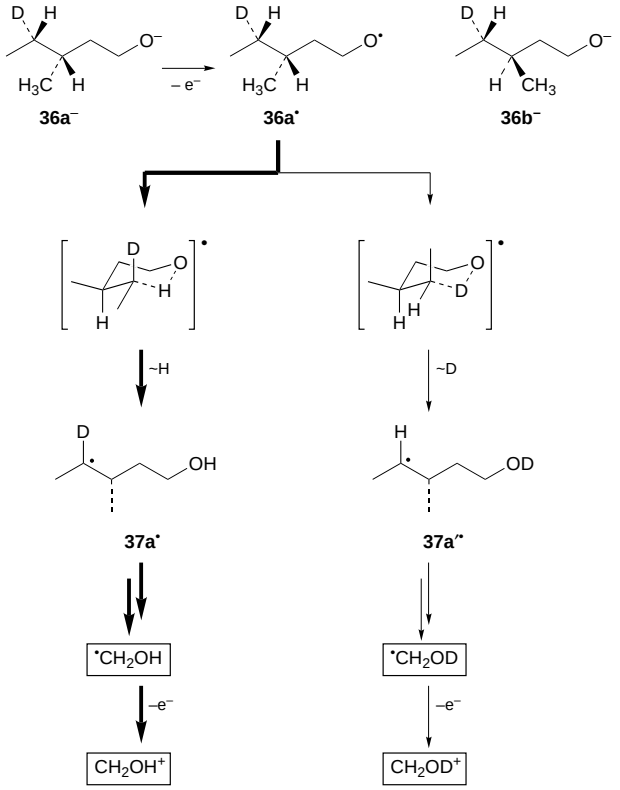

Scheme 6

diastereoisomers show distinctly different ratios of CH_2OH^{+} *versus* CH_2OD^{+} formation, *i.e.* 6.4 : 1 for the isotopologue **36a**$^{-}$ as compared to 0.5 : 1 for the diastereoisomer **36b**$^{-}$. Considering that the only difference between **36a**$^{-}$ and **36b**$^{-}$ is the relative stereochemistry at the C(3) position, the striking diastereoselectivity has to be traced back to a stereochemical differentiation of the transition structures in the course of the 1,5-hydrogen (deuterium) migration. Of course, in addition to a stereochemical effect (SE), the measured CH_2OH^{+}–CH_2OD^{+} ratios for **36a**$^{-}$ and **36b**$^{-}$ are also affected by the operation of a kinetic isotope effect (KIE). Assuming a combined action of a steric and a kinetic effect, it is possible to semi-quantitatively estimate the magnitude of these two effects by applying a simple algebraic approach.[33,40] As a result, from the measured intensities of CH_2OH^{+} and CH_2OD^{+} one can derive the two relevant components, with KIE = 1.8 ± 0.3 and SE = 3.6 ± 1.3 for the 1,5-hydrogen atom transfer in neutral 3-methylpentyloxy radicals.

A straightforward analysis of these results can be accomplished by the mechanism depicted in Scheme 6 for the diastereoisomer **36a**$^{-}$. Upon electron detachment from the anion **36a**$^{-}$, the neutral radical **36a**$^{-\bullet}$ is formed which can subsequently adopt conformations with suitable geometries for the 1,5-hydrogen (deuterium) transfer involving the C(4) position. Thus, two different chair-like transition structures are possible leading to H- and D-atom transfer, respectively. As a result, the carbon centered radicals **37a**$^{\bullet}$ and **37a′**$^{\bullet}$ are formed which subsequently decompose and, after reionization of the neutral hydroxymethyl fragments, yield the corresponding

CH_2OH^+ and CH_2OD^+ cations. For the diastereoisomer **36a**$^\bullet$, the geometry of the TS associated with migration of a hydrogen atom is a chair-like structure in which both methyl substituents adopt favourable equatorial positions. In contrast, deuterium transfer from **36a**$^\bullet$ has to proceed *via* a transition structure, in which one of the methyl groups is forced into the energetically less favourable axial position. However, a theoretical investigation of the *n*-pentyloxy parent system revealed that this model is idealized in that it assumes a perfect chair-like transition structure for the 1,5-hydrogen migration neglecting the partial linearization of the C(4)–H–O moiety (see above). The *Newman*-type representations as depicted in Scheme 7 clarify

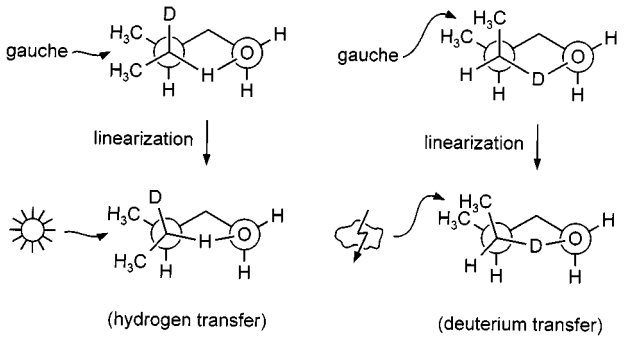

Scheme 7

the influence of this effect. For example, in the transition structure corresponding to the migration of a hydrogen atom (Scheme 6) the 1,2-interactions of the two methyl groups at C(3) and C(4) are reduced upon linearization of the C(4)–H–O subunit. In contrast, for the deuterium shift, these steric interactions are augmented as compared to an ideal chair-like structure. Both pictures, the conformational analysis of chair-like transition structures as well as the description in terms of 1,2-interactions of the methyl groups, predict that the isotopologue **36a**$^\bullet$ will preferentially undergo hydrogen-atom transfer, because this path is favoured by the reduced steric interaction as well as by the kinetic isotope effect, thus giving rise to a large CH_2OH^+–CH_2OD^+ ratio. In contrast, in the diastereoisomer **36b**$^\bullet$, with an inverted relative stereochemistry at the C(3) position, deuterium-atom transfer will be conformationally favoured, but kinetically hampered; consequently SE and KIE almost level out for this stereoisomer as is indeed observed experimentally.

7 Conclusions

The present review article focusses on techniques for the investigation of the chemical reactivity of neutrals generated in NR experiments. As an underlying guideline, a roughly chronological order of the development of these methods has been followed. Parallel to the methodological progress, the chemical systems under study became more and more complex. Beginning with a qualitative examination of simple bond cleavages such as $CH_3CO^\bullet \rightarrow CH_3^\bullet + CO$ and $CH_3Cl \rightarrow CH_3^\bullet + Cl^\bullet$, NR mass spectrometry now allows for the quantitative evaluation of kinetic data, kinetic isotope effects, and even the regio- and stereo-selectivity of a chemical reaction. It is no longer a method for merely probing the existence and structure of elusive neutrals, but has developed to a useful tool for mechanistic studies on the gas-phase reactivity of neutrals in high vacuum.

However, the examination of neutral species with NR techniques is always indirect and remains hampered by a few limitations. (i) As mass analysis of the neutral beam is not possible, the resulting spectrum always consists of a superposition of reactions of both charged and neutral species. (ii) Every NR experiment necessarily involves collisions with target gases. Thus, terms like 'unimolecular' and 'collision induced' become somewhat vague. (iii) In NR experiments, the internal energies of the neutrals do not follow a Maxwell–Boltzmann distribution, which is mentally anchored in and guides intuition of most chemists. Rather, Franck–Condon factors determine the population of electronic and vibrational states. Nevertheless, for the time being the NR methodologies described here in its numerous variants represent the best approach for the generation and examination of many elusive neutrals and their reactivities. If there remain uncertainties as far as the reactivity of a neutral is concerned due to the particular nature of the experiment, a combination of several approaches as discussed above is strongly recommended.

Most of the work presented in this review article took advantage from the synergy of theory and experiment, although this has not been followed in detail here due to the lack of space. It should be stressed that theoretical treatment of the isolated neutrals under study, of the transition structures connecting them, their energies, and their geometries provides a great amount of additional information. Furthermore, questions concerning electronic states, electron affinities, and ionisation energies can be addressed and reaction pathways can be modeled. As the calculations refer to isolated molecules, a direct link to the experiments that are performed in the high-diluted gas phase is established. Thus, theory provides an extremely helpful, complementary tool for the investigation of elusive gaseous neutrals.

In conclusion, as repeatedly demonstrated NR mass spectrometry coupled with computational work has an outstanding potential for the generation and characterisation of unconventional neutrals. With the more recent development of a variety of methods for the investigation of their chemical reactivity, a new field is opened up in this branch of chemistry. The authors of this Review believe that the progress in this field will not only lead to new insight into chemical questions concerning the properties of elusive neutrals, but also to the design of new experimental techniques beyond those described in this contribution.

8 Acknowledgements

We are grateful to Professor C. Wesdemiotis and Professor W. C. Lineberger for communicating some unpublished results and to Professor J. K. Terlouw for helpful discussions. We thank the Deutsche Forschungsgemeinschaft, the Gesellschaft der Freunde der Technischen Universität Berlin, and the Fonds der Chemischen Industrie for financial support.

9 References

1 G. I. Gellene and R. F. Porter, *Acc. Chem. Res.*, 1983, **16**, 200.
2 C. Wesdemiotis and F. W. McLafferty, *Chem. Rev.*, 1987, **87**, 485.
3 J. L. Holmes, *Mass Spectrom. Rev.*, 1989, **8**, 513.
4 A. W. McMahon, S. K. Chowdhury and A. G. Harrison, *Org. Mass Spectrom.*, 1989, **24**, 620.
5 F. W. McLafferty, *Science*, 1990, **247**, 925.
6 F. Turecek, *Org. Mass Spectrom.*, 1992, **27**, 1087.
7 N. Goldberg and H. Schwarz, *Acc. Chem. Res.*, 1994, **27**, 347.
8 D. V. Zagorevskii and J. L. Holmes, *Mass Spectrom. Rev.*, 1994, **13**, 133.
9 R. Haag, D. Schröder, T. Zywietz, H. Jiao, H. Schwarz, P. v. R. Schleyer and A. de Meijere, *Angew. Chem.*, 1996, **108**, 1413; *Angew. Chem., Int. Ed. Engl.*, 1996, **35**, 1317.
10 G. A. McGibbon, J. Hrušák, D. J. Lavorato, H. Schwarz and J. K. Terlouw, *Chem. Eur. J.*, 1997, **3**, 232, and references cited therein.
11 D. Lahem, R. Flammang and M. T. Nguyen, *Chem. Phys. Lett.*, 1997, **270**, 93, and references cited therein.
12 M. J. Polce, Y. Kim and C. Wesdemiotis, *Int. J. Mass Spectrom. Ion Processes*, in press.
13 M. W. Wong, C. Wentrup, E. H. Mørkved and R. Flammang, *J. Phys. Chem.*, 1996, **100**, 10536, and references cited therein.
14 V. Q. Nguyen and F. Turecek, *J. Mass Spectrom.*, 1996, **31**, 843, and references cited therein.

15 R. Feng, C. Wesdemiotis, M. A. Baldwin and F. W. McLafferty, *Int. J. Mass Spectrom. Ion Processes*, 1988, **86**, 95.
16 Review: J. K. Terlouw, *Adv. Mass Spectrom.*, 1989, **11**, 984.
17 M. J. Polce, Š. Beranová, M. J. Nold and C. Wesdemiotis, *J. Mass Spectrom.*, 1996, **31**, 1073.
18 S. Körnig, J. H. M. Beijersbergen and J. Los, *J. Phys. Chem.*, 1990, **94**, 611, and references cited therein.
19 C. E. C. A. Hop and J. L. Holmes, *Int. J. Mass Spectrom. Ion Processes*, 1991, **104**, 213.
20 C. Wesdemiotis, R. Feng, P. O. Danis, E. R. Williams and F. W. McLafferty, *J. Am. Chem. Soc.*, 1986, **108**, 5847.
21 F. Turecek, D. E. Drinkwater, A. Maquestiau and F. W. McLafferty, *Org. Mass Spectrom.*, 1989, **24**, 669.
22 C. Wesdemiotis, B. Leyh, A. Fura and F. W. McLafferty, *J. Am. Chem. Soc.*, 1990, **112**, 8655, and references cited therein.
23 C. A. Schalley, D. Schröder and H. Schwarz, *Int. J. Mass Spectrom. Ion Processes*, 1996, **153**, 173.
24 D. W. Kuhns and F. Turecek, *Org. Mass Spectrom.*, 1994, **29**, 463.
25 M. Sadílek and F. Turecek, *J. Phys. Chem.*, 1996, **100**, 224, and references cited therein.
26 V. Q. Nguyen and F. Turecek, *J. Mass Spectrom.*, 1997, **32**, 55, and references cited therein.
27 M. Sirois, M. George and J. L. Holmes, *Org. Mass Spectrom.*, 1994, **29**, 11.
28 S. A. Shaffer and F. Turecek, *J. Am. Soc. Mass Spectrom.*, 1995, **6**, 1004.
29 S. A. Shaffer and F. Turecek, *J. Am. Chem. Soc.*, 1994, **116**, 8647.
30 F. Turecek, M. Gu and C. E. C. A. Hop, *J. Phys. Chem.*, 1995, **99**, 2278.
31 M. Sadílek and F. Turecek, *J. Phys. Chem.*, 1996, **100**, 15027.
32 M. Sadílek and F. Turecek, *J. Phys. Chem.*, 1996, **100**, 9610; *Chem. Phys. Lett.*, 1996, **263**, 203.
33 C. A. Schalley, *Gas-Phase Ion Chemistry of Peroxides*, Ph.D. Thesis (Technische Universität Berlin, 1997 D 83), Shaker, Herzogenrath/ Germany, 1997.
34 C. A. Schalley, G. Hornung, D. Schröder and H. Schwarz, *Int. J. Mass Spectrom. Ion Processes*, in press.
35 D. W. Boo, Y. Ozaki, L. H. Andersen and W. C. Lineberger, *J. Phys. Chem. A*, 1997, **101**, 6688, and references cited therein.
36 M. M. Bursey, *Mass Spectrom. Rev.*, 1990, **9**, 555.
37 C. A. Schalley, A. Fiedler, G. Hornung, R. Wesendrup, D. Schröder and H. Schwarz, *Chem. Eur. J.*, 1997, **3**, 626.
38 D. Schröder, C. A. Schalley, N. Goldberg, J. Hrušak and H. Schwarz, *Chem. Eur. J.*, 1996, **2**, 1235.
39 D. Schröder, N. Goldberg, W. Zummack, H. Schwarz, J. C. Poutsma and R. R. Squires, *Int. J. Mass Spectrom. Ion Processes*, 1997, **165/166**, 71.
40 G. Hornung, C. A. Schalley, M. Dieterle, D. Schröder and H. Schwarz, *Chem. Eur. J.*, 1997, **3**, 1866.

Paper 7/05838A
Received, 11th August 1997
Accepted, 26th September 1997